www.czasopisma.pan.pl PAN POLSKA AKADEMIA NAUK www.journals.pan.pl

A R C H I V E S O F M E T A L L U R G Y A N D M A T E R I A L S

Volume 59 2014 Issue 3

DOI: 10.2478/amm-2014-0197

H. PAUL*, J. MORGIEL*, T. BAUDIN**, F. BRISSET**, M. PRAŻMOWSKI***, M. MISZCZYK*

CHARACTERIZATION OF EXPLOSIVE WELD JOINTS BY TEM AND SEM/EBSD

CHARAKTERYSTYKA STREFY POŁĄCZENIA UZYSKANEGO METODĄ ZGRZEWANIA WYBUCHOWEGO Z WYKORZYSTANIEM TEM ORAZ SEM/EBSD

The layers near the interface of explosively welded plates were investigated by means of microscopic observations with the use of transmission electron microscopy (TEM) equipped with energy dispersive spectrometry and scanning electron microscopy equipped with electron backscattered diffraction facility (SEM/EBSD). The metal compositions based on carbon or stainless steels (base plate) and Ti, Zr and Ta (flyer plate) were analyzed. The study was focused on the possible interdiffusion across the interface and the changes in the dislocation structure of bonded plates in the layers near-the-interface.

It was found that the extremely rapid temperature increase followed by high cooling rates in the areas near the interface favour the formation of metastable phases. The crystalline or glassy nature of the phases formed inside melted zones strongly depends on the chemical composition of bonded metals. The amorphous phases dominates the melted zone of the (carbon or stainless steel)/Zr whereas the mixture of amorphous phases and nano- grains were identified in (carbon steel)/Ti and (stainless steel)/Ta clads. The elongated shape of the (sub)grains and the randomly distributed dislocations inside them as well as the shear bands and twins observed in the layers near-the-interface of all investigated clads, clearly indicated that during explosive welding, the deformation processes were prevailing over the softening ones.

Keywords: explosive welding, TEM, SEM/EBSD, interface, phase transformations, microstructure

W pracy analizowano zmiany strukturalne oraz składu chemicznego, jakie zachodzą w pobliżu powierzchni połączenia płyt metalowych spajanych z wykorzystaniem energii wybuchu. Badano kompozycje materiałów bazujące na stali węglowej lub stopowej (płyta bazowa) w połączeniu z Ti, Zr lub Ta (płyta lotna). W prowadzonej analizie wykorzystano transmisyjny mikroskop elektronowy (TEM) wyposażony w spektrometr promieniowania X (EDX) a także skaningowy mikroskop elektronowy wyposażony w system pomiaru orientacji lokalnych (SEM/EBSD).

Zaobserwowano, że ekstremalnie szybki wzrost temperatury a następnie szybkie chłodzenie prowadzi do uformowania się w strefie przetopień faz niestabilnych o silnie zróżnicowanym składzie chemicznym. Krystaliczna lub amorficzna natura formujących się faz uzależniona jest od składu chemicznego łączonych metali. Faza amorficzna dominuje w strefach przetopień formujących się w układzie płyt (stal austenityczna lub węglowa)/Zr podczas, gdy mieszanina faz amorficznych i ultra drobnokrystalicznych dominuje w układach płyt (stal węglowa)/Ti oraz (stal astenityczna)/Ta. Analizy strukturalne pokazują, że w warstwach łączonych płyt położonych przy powierzchni połączenia, obserwuje się podstrukturę komórkową z duża ilością dyslokacji zgromadzonych w ich wnętrzu a także bliźniaki odkształcenia (Zr, Ti) oraz pasma ścinania (stal, Zr). Fakty te pozwalają na stwierdzenie, że procesy odkształcenia dominują nad procesami zmiękczenia wywołanymi oddziaływaniem wysokiej temperatury. Udokumentowano także, że pomimo trudności w preparatyce próbek wynikających z silnie odmiennych własności elektrochemicznych łączonych metali, połączenie technik opartych o TEM oraz SEM/EBSD pozwala w pełni opisać zjawiska zachodzące w meso- i nano- skali w pobliżu powierzchni połączenia.

1. Introduction

The application of laminar products as construction elements has significantly increased. It is usually sufficient to apply a thin layer of a material, of highly anti-corrosive properties on a relatively inexpensive base (construction) material to meet the operation requirements, i.e. to obtain element characterized both by high corrosion resistance and strength. High melting materials, such as zirconium, titanium, tantalum, niobium, tungsten, etc., and their alloys, joined on steels perfectly fulfil the above expectations. However, joining these metals with steels still pose a technological problem. That is why, an increase interest in the technology of explosive treatment of materials, including the technology of explosive cladding, is presently observed.

The classic definition of the explosive welding defines it as the process of metal joining in the solid state, as an effect of a collision of joined plates with high velocities caused by

* INSTITUTE OF METALLURGY AND MATERIALS SCIENCE, POLISH ACADEMY OF SCIENCES, KRAKÓW, POLAND
** UNIVERSITÉ PARIS-SUD, ICMMO, CNRS UMR 8182, LABORATOIRE DE PHYSICO-CHIMIE DE L'ETAT SOLIDE, ORSAY, F-91405, FRANCE
*** OPOLE UNIVERSITY OF TECHNOLOGY, FACULTY OF MECHANICS, 5 MIKOŁAJCZYKA STR., OPOLE, POLAND

a controlled detonation of an explosive charge [1, 2]. At the collision point (line), the perfectly clean surfaces are brought together (if the impact angle and the impact velocity are within the range required for bonding) under very high pressure. The high velocity oblique collision will 'produce' high temperature and high shear strain near the collision point in a very short time. This causes local melting of the bonded metals, simultaneously with the local plastic deformation, e.g. [1-7]. Since the process occurs under high pressure and at extremely fast cooling rates, the solidification terms are far from equilibrium, and the occurrence (in the melted zones) of non-equilibrium phases is expected, e.g. [8].

The processes which occur at the interface lead to important structural changes in the subsurface areas of the bonded plates and strongly affect the macroscopically measured 'parameters' characterizing the properties of the clad. In macroscale these changes concern the amplitude and height of the wave being formed and the summarized area occupied by the molten areas. In micro-/nano- scale the changes concern the morphology of the solidified liquid, including their chemical and phase composition, and the changes in the dislocation structure of bonded plates near-the-interface [9]. The very short time of the 'heat influence', due to the high thermal conductivity of the metals, leads to high cooling rates and thus, in the solidification process, the melted metals are usually 'transformed' into brittle intermetallics of different compounds, e.g. [5-7]. These changes are associated with strong and unpredictable (due to intensive mixing in the liquid state under high pressure) changes in the chemical composition within individual melted zones [7].

Despite that, the explosive weld microstructures have been examined for half-a-century, in the literature there is still no agreement on the mechanisms 'controlling' metal bonding during such joining process. In the author's opinion, this results from the 'poorly' investigated processes occurring near the interface. In an earlier works techniques such as: optical microscopy, scanning electron microscopy (SEM) and mechanical testing were used for the microstructural analyses of changes near the interface and the clad properties characterization, e.g. [1-4]. Significantly less publications have been issued on the nano- scale transmisssion electron microscopy (TEM) analyses, especially of the phenomena that occur within the melted zones and the parent metals adhering to the interface. Additionally, they were limited to selected metals compositions, e.g. the steel/Ti clad [10, 11], Ti/Ti clad [12], copper to copper clad [10] or a Ni-based amorphous or metallic glass film clad on stainless steel [13]. Except the works [9-14] on the Al/Cu clad, nothing has been done, to our knowledge, in respect to microstructure characterization by means of SEM/EBSD system.

The present study is focused on the structural changes and the phase transformations occurring at the nano- and microscales inside the bonding zone. Particular attention was paid on the description of the interfacial areas without macroscopically visible melted zones between the bonded plates. Consequently, the reaction products formed in the melted zones were carried out by means of TEM. Next, the microstructure changes that occur close to the interface in explosively welded sheets were analysed by means of a SEM equipped with a high resolution electron backscattered (EBSD) facility. The strongly different electrochemical properties of the bonded metals necessitated the application of the focus ion beam (FIB) technique for the TEM thin foil preparation from the areas covering the interfaces.

2. Materials and experimental procedures

2.1. Materials and explosive cladding process

The plates of zirconium, titanium and tantalum explosively welded with (carbon or stainless) steel plates were analyzed in this study. Sizes of plates were of 300×500 mm^2. A system of parallel arranged plates was applied to manufacture of two-layered clads. The contact surfaces of the joined plates were grounded, cleaned of solid particles and degreased. The detonator was located in the middle of the shorter edge of the flyer plate. In all the cases, in the middle of the plate's width, the jetting direction was parallel to the rolling direction (RD) of the hot rolled sheets. More details of materials and the selected applied process parameters for the particular cases of clad are presented in Table 1. The explosion welded materials evaluated in this study were manufactured by High Energy Technologies Works 'Explomet' (Opole, Poland).

TABLE 1

Selected parameters of explosive bonding

clad	Metals composition: base plates/flyer plate	Applied 'stand-off distance' (mm)	Applied detonation velocity (m/s)	Thickness of welded sheets (flyer/base plate) (mm)	Impact angle (deg)	Collision point velocity (m/s
(Stainless Steel)/ Zirconium	10CrMo9-10/Zr700	4	2200	25/3	12.1	464
(Carbon Steel)/ Zirconium	SA516Gr70/Zr700	6	2200-3500	22/3	10.7 - 16.8	409-643
(Carbon Steel)/ Titaniu	SA516Gr70/Ti(Gr1)	6	2200	22/6	12.4	477
(Stainless Steel)/ Tantalum	10CrMo9-10/Ta	3	2600	12/1.5	17.7	799

2.2. Microstructural and chemical composition analyses

All the samples were cut-off from the 'properly' bonded clad. The nano-/micro scale microstructure observations and the chemical composition measurements were performed by means of a TEM with the use of a FEI Technai G^2 microscope, operating at the accelerating voltage of 200kV. The TEM was equipped with a field emission gun and a high-angle annular dark field scanning/transmission detector (HAADF/STEM), combined with an energy dispersive X-ray (EDX) microanalyser. The resolution of the system for the chemical composition measurements was ~1nm. The Focus Ion Beam (FIB) technique was applied for preparing thin foils along the ND-TD section (where: ND and TD are the normal and the transverse direction, respectively).

The more global microstructural analyses of the interfacial zone (in the same ND-RD section) were performed by means of a SEM, with the use of Zeiss Supra 55VP, equipped with a field emission gun (FEG) and electron backscattered diffraction (EBSD) facility. The microscope control, the pattern acquisition and the indexing were performed with the use of the TSL OIM Analysis 6 software. The orientation maps were created in the beam-scanning mode with the step size ranged between 50nm and 500nm.

3. Results and discussion

At the macro-/meso-scale, the interfaces were outlined by a characteristic sharp transition indicating that there was no mechanical mixing between the welded metals in the solid state. In all the clads the morphology of the joints was characterized by the mixture of wavy and flat patterns, as presented in Fig. 1 for the (carbon steel)/Zr700 clad. The morphology of the joints is strongly affected by explosion velocity and stand-off distance [1-4, 15-17]. The melted zones, if they occurred, were preferentially located near the front slope of the waves or within the vortex of the waves. In some cases, cracks within the brittle melted inclusions were observed. The macro-cracks were situated almost perpendicularly to the interface, whereas micro-cracks (observed only at the SEM or TEM scales) forming non-regular network. It is important to note that the cracks were always limited to the melted zones.

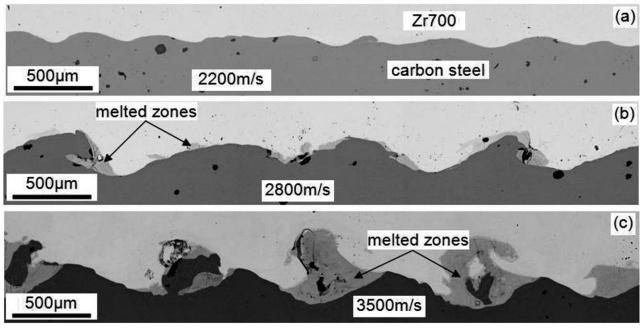

Fig. 1. Morphology of the joint area of plated coatings welded at different detonation velocities: (a) 2200 m/s, (b) 2800 m/s and (c) 3500 m/s characterized using SEM. A constant distance between the plates was used – 6 mm. ND-ED sections

3.1. Microstructure, chemical composition changes and phase constitution inside the intermetallic inclusions. Nano- scale analysis

The rate of the heat transfer, the severe plastic deformation and the high pressure are the most important factors which control the reactions occurring at the boundary between the solid and the liquid phase [8]. From the point of view of the temperature influence, the events taking place during explosive bonding can be attributed to one of the two periods. *In the first period*, the temperature increase is dominant with respect to transferring the heat away from the collision point (which is too slow to be effective). It is widely accepted that the kinetic energy of the jet and the large plastic work of deformation, induce the melting of the materials close to the weld interface [7]. As the process is very fast, there is no time for the heat to be transferred away from the interface, hence any increase of temperature and melting is local. *In the second period* (as the collision point (line) is moved forward), the cooling processes are dominant. During solidification, the melted volumes are subjected to extremely high cooling rates. Consequently, a series of metastable phases (i.e. the phases that do not appear in the equilibrium phase diagram) can be formed [18]. The very short time of the 'impact' of the high temperature caused the melted metals to frequently show a strong tendency to form amorphous phases in the process of solidification. The described processes lead to important structural changes not only inside the melted zones but also in the subsurface areas of the bonded plates (e.g. inside the microstructure of the bonded plates near the interface); these changes strongly affect the macroscopically measured parameters characterizing the properties of the clad, in particular during cyclic loading, e.g. [19]. The changes near the interface for different clads are described below.

3.1.1. Zirconium to carbon or stainless steel composites

Figures 2a and b and 3a are the TEM/BF microstructures of the area near the interface of the (carbon steel (CS))/(zirconium (Zr700)) and (stainless steel (SS))/(zirconium (Zr700)) metal compositions, respectively. The internal microstructures of the broad (a few μm) inclusion and the extremely thin (<50nm) layers were qualitatively similar. The structure composed of nano- grains 'immersed' within the rapidly solidified liquid was the most frequently formed inside the melted zones. The diameter of the nano-grains only rarely exceeds a few tens of nanometers. They were observed as single isolated grains 'immersed' in the solidified melt or as compact chains of grains. However, the crystallization process always preferentially starts from both – (pure metal)/(solidified melt) interfaces. The chemical composition of the phases that form within the intermetallic layers (or inclusions) is strongly diversified, and very often far from the phases observed on the equilibrium phase diagram, i.e. starting from Zr→Fe: Zr_3Fe, Zr_2Fe, $ZrFe_2$ or $ZrFe_3$ (in the case of the CS/Zr clad) and, e.g. $Fe_{21.8}Zr_{75.0}Ni_{1.8}Cr_{1.4}$ and $Fe_{72.0}Zr_{26.4}Ni_{0.0}Cr_{1.6}$ (for SS/Zr).

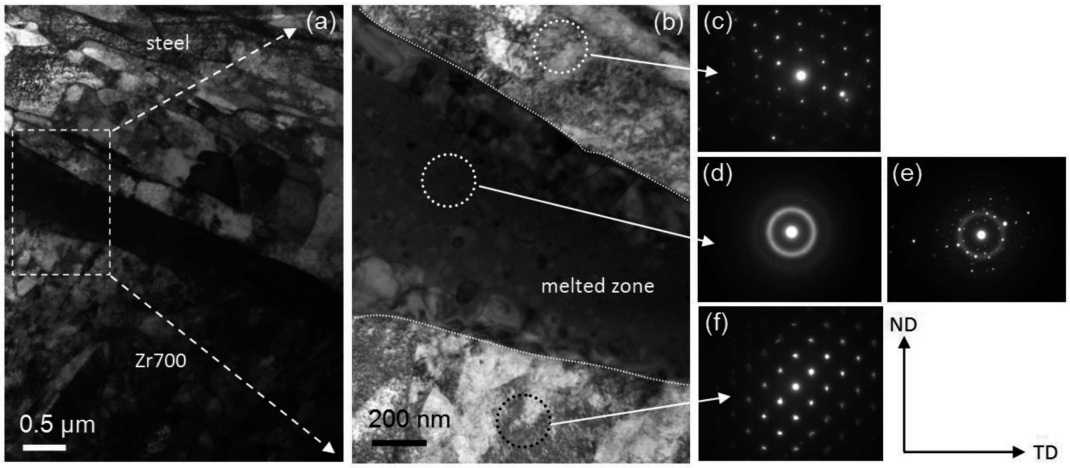

Fig. 2. TEM/BF images presenting microstructure of an interfacial area of the (carbon steel)/Zr700 clad produced with the detonation velocity of 3500 m/s: (a) of the joint area including the Zr layers, the melted zone and the carbon steel layer, (b) detail from (a) showing the inside of the melted zone and the formation of amorphous and ultrafine grains. (c)-(f) SAD patterns from the area of: (c) steel, (d) and (e) solidified liquid confirming its partly amorphous nature and (f) Zr700

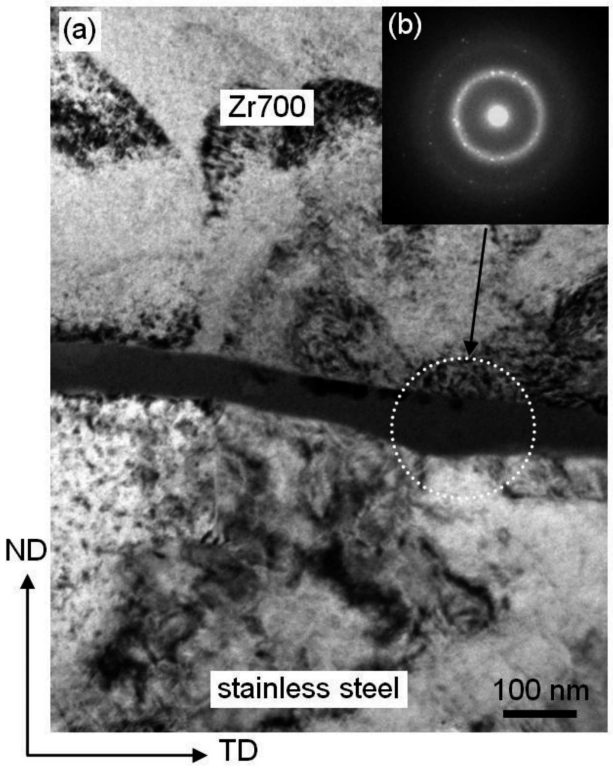

Fig. 3. TEM bright field image presenting microstructure of an interfacial area of the (stainless steel)/Zr700 clad: (a) the joint area including the Zr layers, the melted zone and the carbon steel layer, (b) SAD patterns from the area of solidified liquid confirming its amorphous and ultra-fine grained nature

3.1.2. Titanium to carbon steel composite

Figures 4a and b are the HAADF/STEM microstructures of the area near the interface of the CS/Ti metal composition. The melted zone between Ti and CS plates was ~6 μm thick and their interior is composed of very fine grains with the diameter mostly ranged between 150 nm and 200 nm. Some of the grains resemble small dendrites with a clearly marked core and arms. Generally, the grains showed a typical crystalline contrast during tilting in TEM, but very often neighbouring thin areas were amorphous. (This can be deduced from the slightly marked ring on the diffraction pattern from the area of grains, as visible in the SAD pattern of Fig. 4). A similar structure of the melted zone interior was also observed by Song et al [6] for the same type of (carbon steel)/Ti clad. Near the both interfaces (of the (melted zone)/(pure metal)-type) a structure of coarse or even columnar grains was observed. The chemical composition of the phases that form within this melted zone is roughly homogeneous and can be described as ~Fe_2Ti_3.

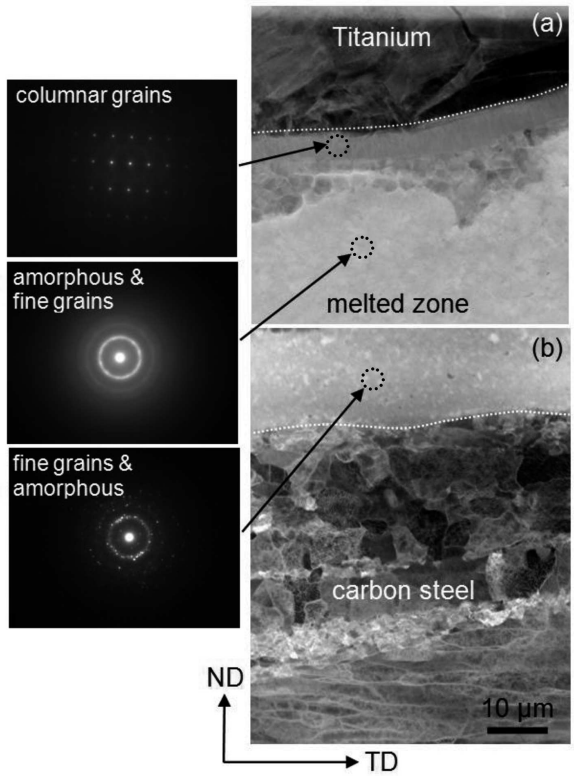

Fig. 4. HAADF/STEM images presenting microstructure of the melted zone and the areas of the joined metal sheets which directly adhere to: (a) Ti/(melted zone) and (b) (melted zone)/(carbon steel) interface and corresponding particular areas the SAD patterns. The (carbon steel)/Ti clad

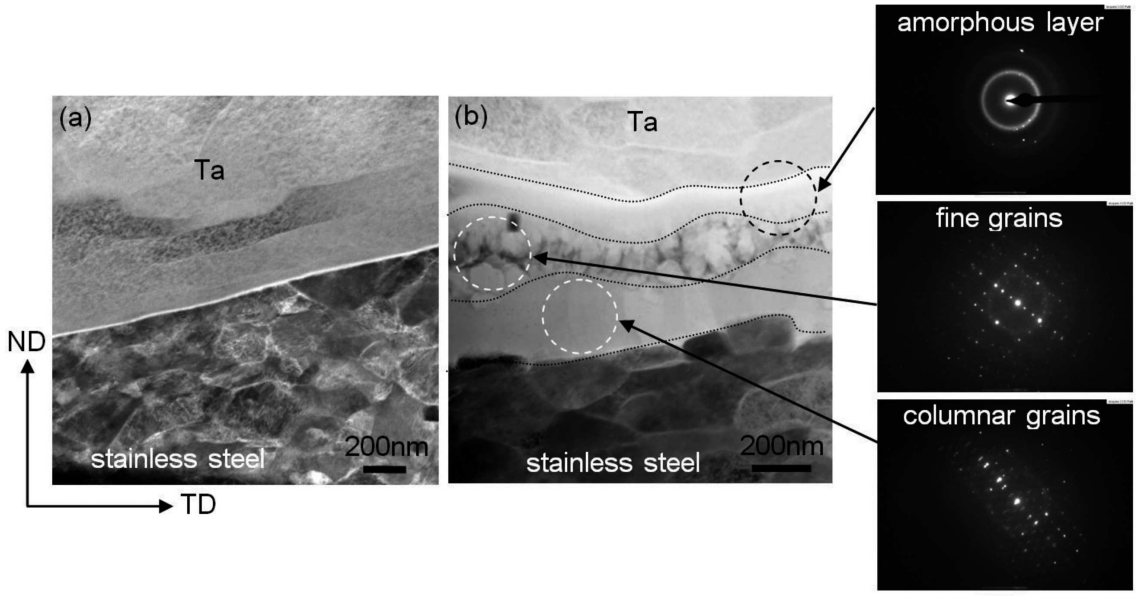

Fig. 5. HAADF/STEM images presenting microstructure of the melted zone and the areas of the joined metal sheets which directly adhere to: (a) extremely thin and (b) thin melted zones, formed between Ta and stainless steel plates and corresponding particular areas the SAD patterns. The (stainless steel)/Ta clad

3.1.3. Tantalum to stainless steel composite

The HAADF/STEM microstructures of the (stainless steel)/tantalum clad, in the near-the-interface areas, are presented in Figs. 5a and b. Microstructures show extremely thin (<20 nm) and thin (~500 nm) melted zone formed between welded plates. The layers inside the melted zones are either totally amorphous, crystalline, or form a mixture of both these phases. In some cases, the new grains that nucleate within the solidified melt take the form of dendrites, with a well-developed core and arms. For the case presented in Fig. 5b, an amorphous layer of ~200 nm thick is adhering to the Ta sheet, whereas the layer of ~500 nm thick, directly adhering to the steel sheet, is crystalline. The chemical compositions of particular layers were different and most of the observed phases were far from equilibrium, i.e. the phases were not observed on the equilibrium phase diagram. The TEM/EDX measurements show, that starting from Ta sheet across the interface, the chemical composition changes within the molten zone are as follows: $Fe_{46.2}Ta_{41.2}Cr_{12.6} \rightarrow Fe_{48.3}Ta_{30.9}Cr_{13.9}Ni_{6.9} \rightarrow Fe_{60}Ta_{11.3}Cr_{16.6}Ni_{12} \rightarrow Fe_{71.3}Ta_{1.4}Cr_{23.7}Ni_{3.6}$.

3.2. Microstructural changes in base metals near the interface

3.2.1. Dislocation structure

The dislocation structures in the layers near-the-interface, independently of the analyzed clad, were qualitatively similar. In all the bonded materials, a well-defined cellular dislocation structure was observed. At the micro-/nano- scale, the layers of the base metals adhering to the interface show typical deformed microstructure features, i.e. structure refinement, elongated dislocation (sub)grains or slip bands and, in some cases, micro twins (in Ti, Zr or SS) or shear bands (CS, SS, Ti or Zr). In all cases, the fine grained structures formed near the interface were elongated parallel to the impact direction. The elongated grains within the wavy region (mainly in the crest of the waves) took a characteristic shape reflecting the rotational character of the material displacement, as observed earlier for the Al/Cu clad [9, 14]. The dislocation structure in layers near the interface is composed of elongated regular dislocation arrangements (forming (sub)grain boundaries) and randomly distributed dislocations within particular (sub)grains. The (sub)grain length was in order of a few microns, whereas their width – a few tens or hundreds of nanometers. (However, it could be noted that the TEM/BF imaging counts all the types of boundaries, i.e. low- and high- angle, without distinction). The elongated shape of the (sub)grains and the randomly distributed dislocations inside them clearly indicates that, during welding, the deformation processes were prevailing over the softening ones.

3.2.2. Structural changes analysed by SEM/EBSD system

The microstructure across the interface were characterized in meso- scale by means of the SEM/EBSD local orientation measurements. Two characteristic places within the samples in the 'as bonded' state, i.e. the areas located across the interface with melted zone and the areas placed near the interface where the melted zone was very thin or (macroscopically) not observed, were analyzed in detail.

Figures 6-8 show the orientation maps made across the interface and presented as a 'function' of the band contrast and phase component maps. The 'band contrast' maps clearly reveal the differences observed in the microstructure of both welded metals. The structure of the plates near the interfaces was composed of deformed grains elongated along RD. However, this directionality in the grain geometry (in both metals) was lost as the distance from the interface increased. Finally, in the areas distanced about 100 μm from the interface, nearly globular grains were observed, but still with the increased density of the dislocations (marked as low angle grain boundaries) inside the grains' interior.

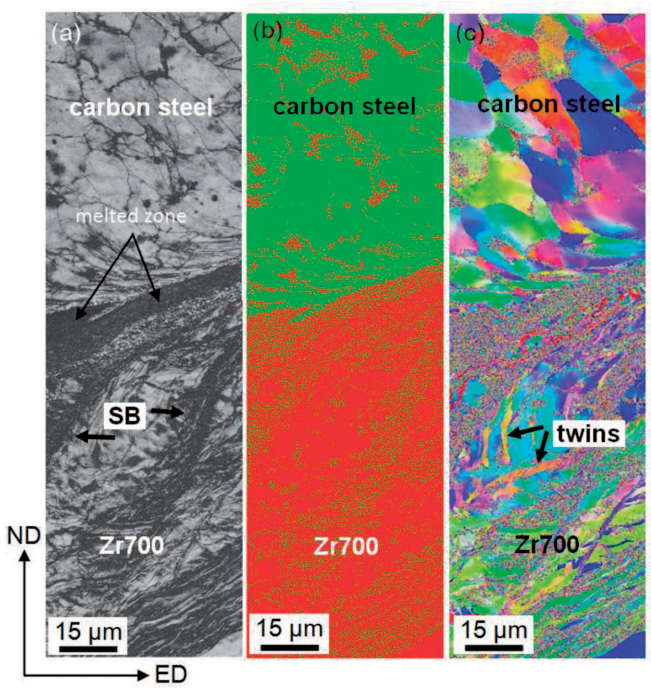

Fig. 6. Orientation maps displayed as a 'function' of (a) band contrast, (b) phases distribution, and (c) inverse pole figure colours of near-the-interface area of (carbon steel)/Zr700 clad. SEM/EBSD local orientation measurements with the step size of 100nm

The formation of the extremely fine-grained structure near the interface is the common characteristic feature observed in all welded sheets. In the case of Ti and Ta the thickness of the fine-grained layer was a few micron, whereas in the case of steels and Zr at least of few tens of microns. The strongly refined structure is especially well-visible inside the areas of the waves. The crest of the waves was always composed of very thin (with the thickness below 200 nm) and elongated grains, separated by large angle grain boundaries. These thin grains were strongly curved inside the crest of the wave and imitated well the rotational character of the material displacement during the wave formation, i.e. reflecting the non-homogeneous flow close to the interface.

The 'intensity' of the plastic deformation decreases as the distance from the interface increases, as observed earlier in, e.g. [1, 2, 7, 16]. In the areas placed 'far' from the interface, the grains are nearly equiaxed and their interior is characterized by only a slightly increased density of the dislocations. In all metals the dislocation slip led to well-defined dislocation cells, as typically observed in the cold-rolled (up to moderate strains) sheets; both equiaxed and elongated cells were observed. The mechanism of deformation by slip was supported in some areas of the Zr and Ti by deformation twinning, i.e. thin deformation twins occurring against the background of the dislocation cells and by shear banding especially well visible in steels and Zr.

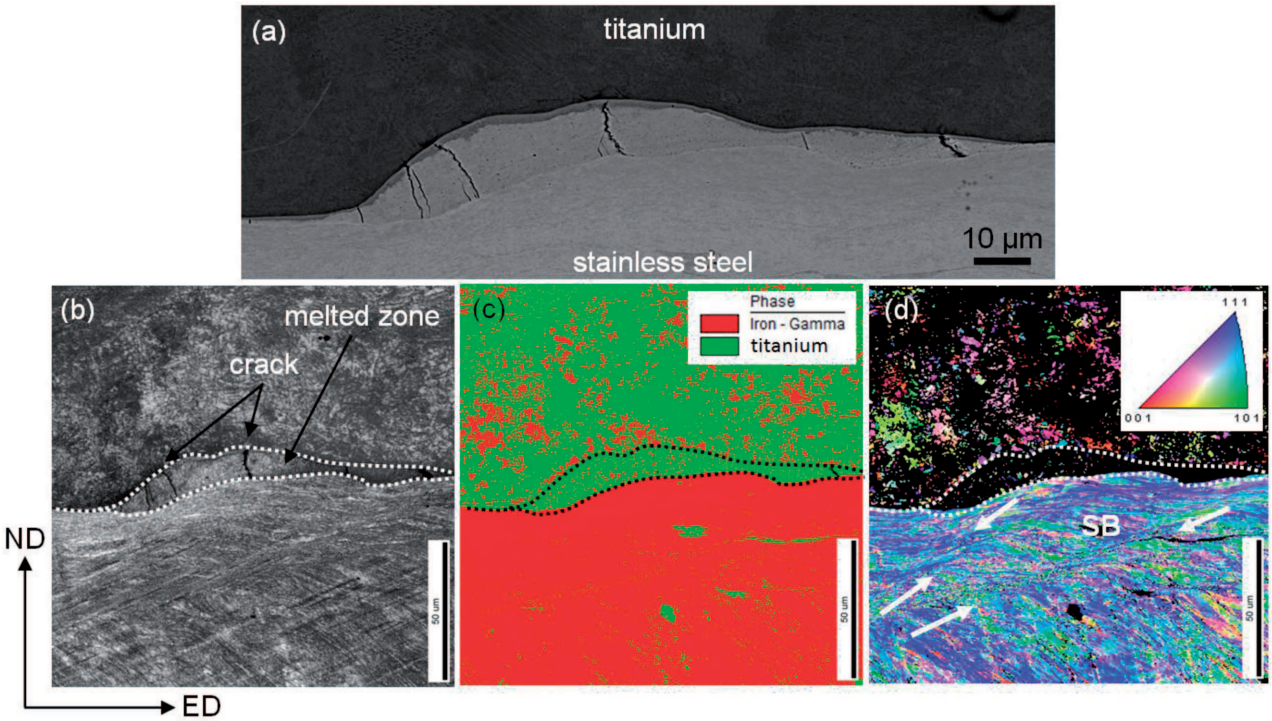

Fig. 7. Orientation maps displayed as a 'function' of (a) band contrast, (b) phases distribution, and (c) inverse pole figure colours of near-the-interface area of (stainless steel)/Ti clad. SEM/EBSD local orientation measurements with the step size of 100nm

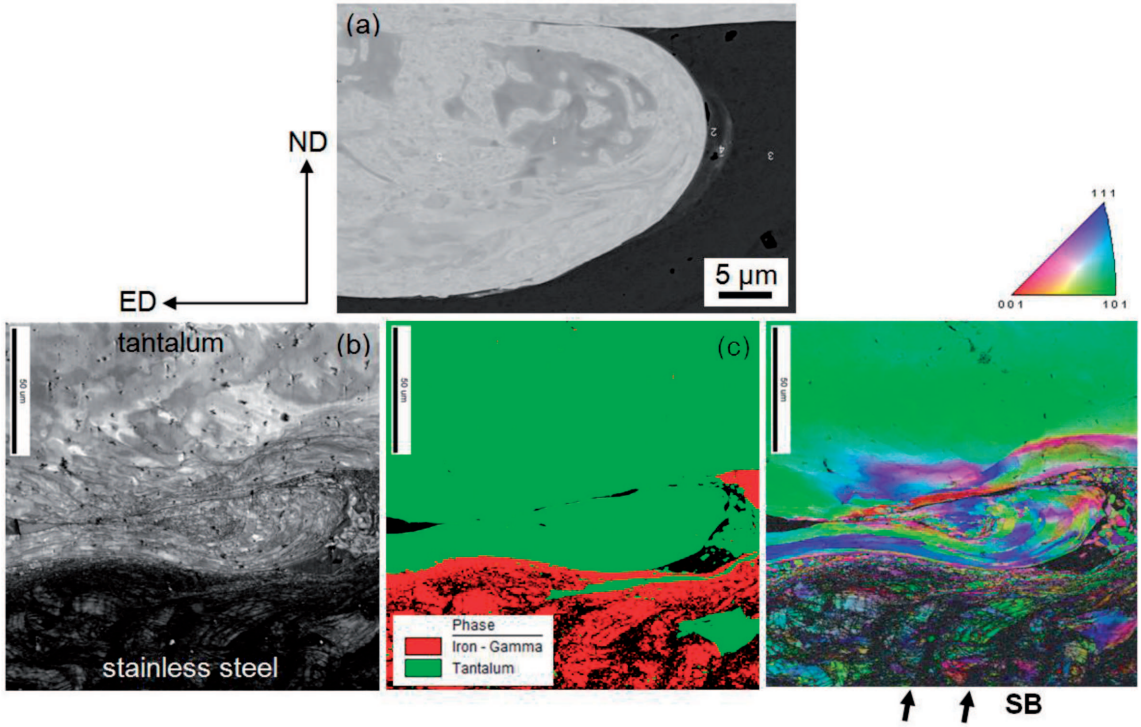

Fig. 8. Orientation maps displayed as a 'function' of (a) band contrast, (b) phases distribution, and (c) inverse pole figure colours of near-the-interface area of (stainless steel)/Ta clad. SEM/EBSD local orientation measurements with the step size of 100nm

4. Summary

This work describes the nano- and meso- scale analyses of the microstructure and the chemical composition changes that occur in the interfacial layers of explosively welded sheets. The clads based on stainless or carbon steels as base plates and Ti, Zr or Ta as flyer plates were analysed in detail. The following conclusions can be drawn.

- 'Metallurgical bonding' was achieved by a melting of the explosively welded sheets. The above proves that the proper explosive welding always incorporates the melting of thin surface layers of joined materials.
- The amorphous phases and the nano- grains were identified in the melted zones placed near the interface in all analysed cases. The quantity of crystalline or amorphous phases in the solidified melt strongly depends on the chemical composition of the bonded sheets.
- During the bond formation, the layers of parent sheets near the interface underwent intense plastic deformation. Consequently, the deformation microstructure features, i.e. the elongated shape of the (sub)grains and the randomly distributed dislocations inside them, the deformation twins (in Ti, Zr) and the shear bands (steels and Zr) were observed. This clearly indicates that, during welding, the deformation processes were prevailing over the softening ones.

Acknowledgements

This work was supported in part by the National Science Centre (Poland) under Grants number: UMO-2012/05/B/ST8/02522 and UMO-2012/04/M/ST8/00401.

REFERENCES

[1] T.Z. Blazynski, Explosive Welding, Forming and Compaction, Applied Science Publishers LTD, New York, 1983.
[2] H. Dyja, A. Maranda, R. Trębiński, Technologie wybuchowe w inżynierii materiałowej, Wydawnictwo WMiIM Politechniki Częstochowskiej, Częstochowa 2001 (in polish).
[3] S.A.A. Akbari Mousavi, S.T.S. Al-Hassani, A.G. Atkins, Materials and Design **29**, 1334-1352 (2008).
[4] F. Findik, Materials and Design **32**, 1081-1093 (2011).
[5] Y. Yang, B. Wang, J. Xiong, J. Mat. Sci. **41**, 3501-3505 (2006).
[6] J. Song, A. Kostka, M. Veehmayer, D. Raabe, Mat. Sci. Engn. **A528**, 2641-2647 (2011).
[7] H. Paul, L. Lityńska-Dobrzyńska, M. Prażmowski, Metall. Mater. Trans. A **44A**, 3836-3851 (2013).
[8] K.F. Kelton, A.L. Greer, Non-Crystalline Solids **79**, 295-309 (1986).
[9] H. Paul, M. Miszczyk, M. Prażmowski, Mat. Sci. Forum **702-703**, 603-606 (2012).
[10] S.H. Carpenter, in., Shock Waves and High-Strain-Rate Phenomena in Metals, eds. M.A. Meyers, L.E. Murr, Plenum Press, New York, 941-959 (1981).
[11] D.G. Brasher, D.J. Butler, A.W. Hare, in., Shock Waves for Industrial Applications, ed. L.E. Murr, Noyes Publications, 216-23 (1988).
[12] Y. Yang, B. Wang, J. Xiong, J. Mat. Sci. **41**, 3501-3505 (2006).
[13] K. Hokamoto, K. Nakata, A. Mori, S. Ii, R. Tomoshige, S. Tsuda, T. Tsumura, A. Inoue, Journal of Alloys and Compounds **485**, 817-821 (2009).
[14] H. Paul, L. Lityńska-Dobrzyńska, M. Miszczyk, M. Prażmowski, Arch. Metall. Mater. **57**, 1151-1162 (2012).
[15] M. Prażmowski, H. Paul, D. Rozumek, E. Marcisz, Key Engineering **592-593**, 704-707 (2014).

[16] M. Prażmowski, H. Paul, F. Żok, Rudy i Metale Nieżelazne R58 (2013) pp. 644-651 (in polish).
[17] N.V. Naumovich, A.I. Yadevich, N.M. Chigrinova, in., Shock Waves for Industrial Applications, ed. L.E. Murr, Noyes Publications, 170-215 (1988).
[18] H. Paul, M. Prażmowski, J. Morgiel, M. Faryna, W. Skuza, Rudy i Metale Nieżelazne R58 (2013) pp. 603-610 (in polish).
[19] A. Karolczuk, M. Kowalski, R. Bański, F. Żok, Experimental Mechanics **48**, 101-108 (2013).

Received: 20 March 2014.